

INVENTORY OF LANDSLIDES TRIGGERED BY HURRICANE MATTHEWS IN GUANTÁNAMO, CUBA

Georgui B. Posphehov¹, Yasmira Savón^{1*}, Ricardo Delgado², Enrique A. Castellanos³, Arisleydis Peña⁴

¹ Saint Petersburg Mining University. 21-Ya Liniya Vasil'yevskogo Ostrova, 2, St Petersburg, 199106.

² Delegation of the Ministry of Science, Technology and Environment, Ahogados e/ 12 y 13 north. No. 14. Guantánamo, Cuba.

³ Ministry of Energy and Mines, Ave. Salvador Allende #666, Centro Habana, La Habana, Cuba.

⁴ Institute of Meteorology. Meteorological Center of Guantánamo. 13 North # 14 e/ 1 y el 2 west, Reparto Caribe, Guantánamo, Cuba.

*Corresponding author: yusmirasvaciano@gmail.com

Received: September 16th, 2022 / Accepted: February 15th, 2023 / Published: March 31st, 2023

<https://DOI-10.24057/2071-9388-2022-133>

ABSTRACT. Hurricane Matthew affected the eastern region of Cuba from October 4th to 5th causing large damages and numerous landslides. This research presents an inventory of landslides triggered by the hurricane. Visual interpretation of satellite images of moderate resolution from Sentinel 2A instrument and localized higher resolution satellite images provided by PlanetScope, as well as field research were the main sources of information. The resulting landslide inventory was compared with other landslide factors such as slope, geology, and soil deep and composition from maps at a scale of 1:100 000. Data recorded by 1-hour rain gauges and 24-hour rain gauge was also analyzed in order to identify rainfall thresholds for the occurrence of landslides during the Hurricane Matthew influence in the study region. A total of 619 landslides were identified and classified as rockslide, rockfall or debris flows. The research found the slope was not as important factor as the type of rock. Most of landslides were located in areas of green shale of volcanic and vulcanoclastic rocks and rocks of the ophiolitic complex formed by ancient remnants of oceanic crust. The accumulate rainfall threshold estimated for the event was between 178-407 mm/day.

KEYWORDS: Landslide inventory, Hurricane Matthew, Rainfall Threshold, Guantánamo

CITATION: Posphehov G. B., Savón Y., Delgado R., Castellanos E. A., Peña A. (2023). Inventory Of Landslides Triggered By Hurricane Matthews In Guantánamo, Cuba. *Geography, Environment, Sustainability*, 1(16), 55-63

<https://DOI-10.24057/2071-9388-2022-133>

Conflict of interests: The authors reported no potential conflict of interest.

INTRODUCTION

Landslides are very dangerous geomorphological phenomena that cause damage to social infrastructure, making it ineffective, and to economic infrastructure, contributing to a decrease in productivity, hence the importance of their study and prediction (Kutepova 2012). These phenomena are closely linked to the physical-mechanical properties of the rock masses, which determine the degree of deformation of these (Gospodarikov 2010; Gusev 2016; Posphehov et al. 2018; Trushko and Protosenya 2019) and also to conditioning factors such as the type of rock, topography, soil characteristics, hydrogeology (Dashko 2018; Kutepova 2012), the rain among others.

A significant part of the methodologies for landslide risk assessment includes as a fundamental input, detailed information on the previous occurrence of landslides in the study area (Dai et al. 2001; Ayalew and Yamagishi 2005). Which strengthen the case for comprehensive landslide inventories as requirement to quantify both landslide hazards and risks (van Westen et al. 2008). Research on landslide inventories has been conducted at global (Brown et al. 1992), as well as nation or regional levels (Guzzetti et al. 1994 and Marcelino et al. 2009).

Landslides induced by tropical cyclones are a significant threat to lives and property in the Caribbean basing

(Bertinelli, Mohan, and Strobl 2016). Furthermore, due to the global climate trends, the frequency and intensity of those atmospheric phenomena are bound to increase (Kleptsova et al. 2021). Such increases in tropical cyclone activity pose increasing risks even for extra tropical areas usually considered outside their reach (Ranson et al. 2014). These conditions require frequent updating of landslide inventories in order to gain better comprehension of the landslide hazards and risks.

The island of Cuba is the largest of the Caribbean region with 109 884 km². Its eastern region is the most prone to the occurrence of landslides, due to the abundance of mountainous areas with steep slopes. Most of landslides are associated with meteorological events such as tropical cyclones or prolonged periods of rain (Castellanos and van Westen 2008). Landslide hazard, vulnerability and risk assessments carried out in Guantánamo province as part of the national effort to improve disaster management, among other research (Castellanos and van Westen 2007) concluded that rainfall is the most important triggering factor for landslide events in the area.

The year 2016 was very active from the meteorological point of view for the easternmost region of Cuba due to several events that caused heavy rainfall. In the proposed study area there were 19 heavy rainfall events (more than 100 mm in 24 hours) recorded by the rain gauge network

maintained by the Institute of Meteorology and the Institute of Hydraulic Resources. Two months recorded the heaviest rainfall: April with five heavy rainfall events accumulating 863.3 mm and October with 12 heavy rainfall events accumulating 2448.6 mm. In this work we present the inventory of landslides triggered by hurricane Matthew as it passed through the eastern part of Cuba.

The landslide inventory was carried out for the period from August 2016 to January 2017. The main source of information for this inventory were before and after the event Sentinel 2A satellite images from MSI instrument operated by the European Space Agency (ESA). Moderate resolution (10 m per pixel) true color and false color near-infrared images were generated from level 1C products. Images dates, identifiers and cloud percentage are shown in Table 1. Before and after hurricane images provided by PlanetScope were also used for the areas where the occurrence of landslides was more frequent. PlanetScope images have a mean resolution of 3 m per pixel of which true color and false color near infrared scenes were used. Scene dates, identifiers and cloud percentage are shown in Table 1.

As can be seen in the Table 1, Sentinel images covered the period before and after the hurricane from August 30, 2016 to January 1, 2017. These images covered the entire study area. PlanetScope images were used in an area of 5 000 km² in total. The selection of scenes was conditioned by the cloud percentage, which interferes with the visual analysis by the selected period in which there was no episodes of intense rains that could cause landslides unrelated to the hurricane.

The limits of the study area were defined taking into account the frame of topographic sheets at 1:10 000 scale. High-resolution post event satellite images provided by free internet providers Google and Microsoft were used as additional source of information.

The study area was divided into 183 squares of 5 × 5 km and a visual interpretation was made using true color, false color infrared and Normalized Difference Vegetation Index (NDVI) scenes to enhance the discrimination of areas with vegetation coverage. Each square was examined and searched looking for vegetation loss and soil and rocks exposed after the hurricane and for typical landslide fans and features. Points were drawn near the center of suspected landslides for further review.

After the visual interpretation phase, field visits were made to selected locations in the study area for the purpose of checking and direct identification of landslides.

Table 1. Satellite images used in the landslide inventory after the passage of Hurricane Matthew on October 4, 2016

Satellite image	Date/Time	Cloud Percentage
Sentinel 2A	2016-08-30 T15:36:22.026Z	36.68
Sentinel 2A	2016-09-19 T15:36:12.026Z	6.60
Sentinel 2A	2016-10-09 T15:36:12.026Z	40.77
Sentinel 2A	2017-01-07 T15:36:01.026Z	9.81
PlanetScope	2016-10-22 T08:07:49Z	11
PlanetScope	2016-10-19 T14:31:14+00:00	6
PlanetScope	2016-10-19 T14:31:15+15:00:00	14
PlanetScope	2016-10-19 T14:31:16+00:00	6
PlanetScope	2016-10-19 T14:31:17+00:00	4
PlanetScope	2016-10-19 T14:31:18+00:00	0

Some of the fieldwork was focused to confirm areas of possible occurrence of landslide events. Several fieldwork routes were traced through the towns and roads affected by the hurricane.

Once the landslide inventory was completed, spatial analysis was used to preliminarily identify the main environmental factors associated with landslides in the area. These analyzes comprise maps of elevations and slopes derived from a digital elevation model (DEM) with a resolution of 25 m per pixel, where the slope in degrees and the elevation in meters above sea level were analyzed. The vertical uncertainty DEM is in a range of 10 m. Likewise, the geological map at a scale of 1:100 000 from the Institute of Geology and Paleontology and the soil parameters (soil depth and texture) at a scale of 1:100 000 from the Institute of Soils of Cuba were included in the analysis.

In order to better understand the behavior of the rain as a triggering factor, the precipitation data from 1-hour rain gauge stations operated by INSMET and 24-hour rain gauge stations operated by INRH. Data was collected for the year 2016 and for October 2016. Analysis of rainfall thresholds that contributed to the occurrence of landslides during the passage of Hurricane Matthew was carried out, taking into account accumulated rainfall data.

The expression for threshold (Th) calculations proposed by (Stedinger et al. 1993) was used in this research. This expression excludes high and low values that are far from the central tendency of the sample:

$$Th = X^- \pm k_n S_y \quad (1)$$

where X^- and S_y are the mean and standard deviations of the logarithms of accumulated rainfall peaks, excluding previously detected outliers, and k_n is a critical value for the sample size n whose data points deviate significantly from the trend of the remaining data. Its expression is the following

$$k_n = -0.9043 + 3.345\sqrt{\log n} - 0.40461\log n \quad (2)$$

For normal data, the largest observation will exceed $X \pm k_n S_y$ with a probability of only 10 percent; therefore, the equation is a one-sided test for outliers with a significance level of 10 percent, for a normal distribution; k_n values are tabulated for samples $n > 150$

For this expression, low outliers are generally valid observations, but because the logarithms of the observed rainfall accumulation peaks are used to fit a two-parameter distribution with a generalized coefficient of deviation, one or more unusual values may distort the entire fitted frequency

distribution. Therefore, detection of such values is important, and fitted distributions should be compared graphically with the data to detect problems (Stedinger et al. 1993).

Study area

The area of influence of Hurricane Matthew is located in the eastern of Cuba (Fig. 1). Low mountains with less 600 meters above sea level (masl) predominate in this area. There are also some relatively isolated heights not exceeding 1200 masl. Coastal plains and small intra-mountains alluvial valleys surrounded by steep slopes are the most common flat areas in the region (Figure 1a).

The study area is complex from the lithological and structural point of view. It is composed of the rocky complexes of the Cretaceous basement, with rocks of the metamorphic complex, mainly sericite and albite schists and andesite-basaltic lavas. The layers are finely stratified and rocks of the ophiolitic complex have a high degree of fracturing. There are also rocks of the Paleogene volcanic island arc with predominance of tuffs. To a lesser degree, there are rocks of the Neogene-Quaternary coverage composed mainly by the alternation of sandstones, lutite, calcareous lutite and biotrititic limestones (Iturralde-Vinent 1998). The marine terraces are composed of bioclastic and biogenic limestone, calcareous sandstone generated by a combination of recent movements of the earth's crust with the cycles of sea levels due to glaciations stand out in the coastal area. The mountain ranges in the area represent one of the most extensive and well-preserved forest ecosystems in the Antilles.

Matthew Hurricane

Hurricane Matthew, which hit the northeast of the island of Cuba, originated as a tropical storm from a strong tropical wave south of the Lesser Antilles in the early morning of September 28, 2016, reaching category 5 on the Saffir - Simpson scale on October 2 in the warm waters of the eastern Caribbean. It made landfall in Cuban territory on October 4 approximately at 6:00 p.m. in local time near Punta Caleta (20°07'00" N, 74°30'10" W), on the south coast as a category 4 in Saffir-Simpson scale (Ballester and Rubiera 2016) as shown in Figure 1b.

Hurricane Matthew has been the most intense recorded in this region of Cuba and caused damage to agriculture, communications infrastructure, electricity, water supply services, roads and homes in the affected communities. Total economic losses were estimated at 2,430.8 million pesos, of which 24.1 million were spent on prevention measures, 388.5 million on home reconstruction, 70.1 million on equipment, 519.5 million in the agriculture and 81.9 million in goods and services, according to data from the National Statistics Office. It should be noted that the data available on hurricane damage in Cuba is generally not differentiated by cause, which makes it difficult to identify the proportion of those losses caused by landslides.

Figure 2a presents the accumulated rainfall of the stations during the year 2016. It is notable the increase in the accumulated precipitation recorded in stations d1, h6, h3, d2 and d3 in October, coinciding with the occurrence of hurricane Matthew. Gauges d1, d6 and h3 recorded the highest accumulated rainfall in the year in this time period totaling 2309.2 mm; 2217.3 mm and 1690.6 mm in the year respectively.

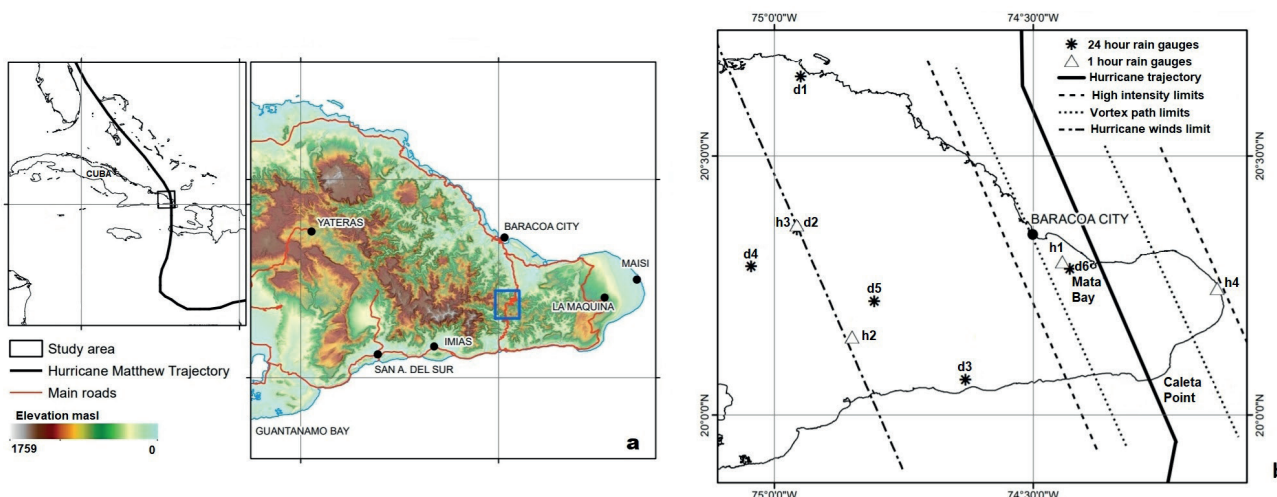


Fig. 1. a) Location of Study Area, hurricane Matthew track and elevation. b) Affected zone of hurricane Matthew and rain gauge location (after Ballester and Rubiera, 2016; and Steward 2017). The blue box in 1a correspond to the photos of Figure 3.

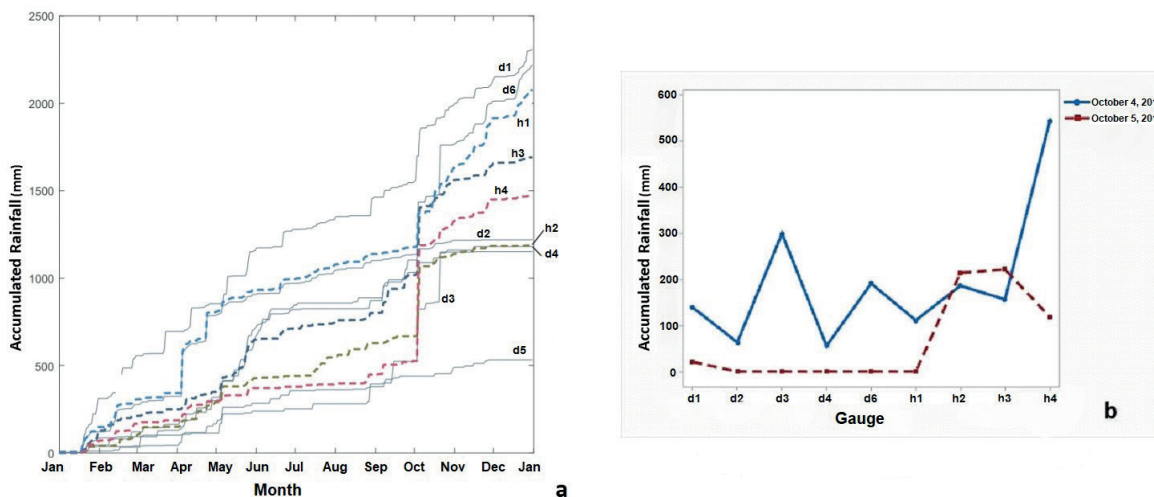


Fig. 2. a) Accumulated rainfall recorded by 1-hour (dashed line) and 24-hour (straight line) rain gauge stations in 2016. b) Accumulated rainfall recorded by each gauge on October 4th and 5th

The highest accumulated rainfall due to Hurricane Matthew was recorded by gauges h4, h2 and h3 (located in Figure 1b). October 4th was the day of highest precipitation in the entire area affected by the hurricane as shown in (Figure 2b). The heavy rainfalls associated with the hurricane and its feeding bands were very intense, specifically on the days of Hurricane Matthew. Rainfall peaked on the day 4 in the gauges h4 and d3 and on the day 5 in gauges h2 and h3. It must be noted that several gauges ceased to operate after October 4th due to the hurricane damages to equipment and infrastructure.

Results and discussion

The inventory carried out in the study area found 619 landslide events associated to Hurricane Matthew. Those

landslides were identified taking into the time frame, selecting only recent material movement with loss of the soil layer. The vast majority of those landslide events were shallow landslides. The Figure 3 shows typical landslide examples among those selected.

The identified landslides were classified according to Keefer and Wilson (1989) as rockslides, debris flows and rockfalls. Rockfalls and debris flows corresponding accounted to 86 % of identified landslide events and concentrated at the north and center of the study area as shows Figure 4a. Rockfalls were only identified in the southern part of the study area near marine terraces, which is consistent with previous research (Castellanos & Van Westen, 2008) see Figure 4a.



Fig. 3. Landslide photos taken on 27.11.2016 during fieldwork. Photo location in the blue box in figure 1a

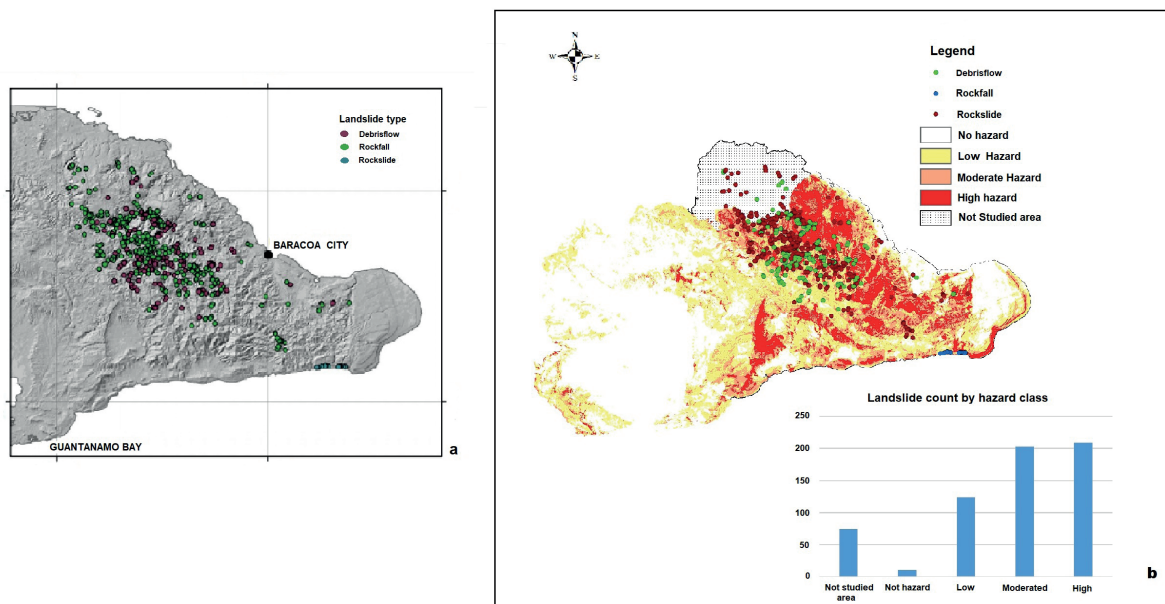


Fig. 4. Landslides triggered by hurricane Matthew. a) Landslide inventory on the relief map and b) Landslides inventory on the hazard map (Castellanos & van Westen, 2008)

Comparing the new inventory of landslides with a previous landslide hazard map for Guantanamo province (Castellanos & Van Westen 2008), 75% of landslide events occurred in area classified as of moderated and high landslide hazard (202 and 209 events respectively) while only 23% (123 events) were located in areas classified as low hazard areas and 2% in not hazard areas (Figure 4 b). Landslides outside the landslide hazard map were not taken into account. This result validates the rationale under the cited research and offers insight into better addressing the hazard mapping in the region.

The spatial analysis of the relation between the landslide inventory and geographical and geological factors found that slope angle is very important component of the conditioning factors as mentioned by Aristazabal and Gómez (2007) and Aristizabal and Yokota (2006). This research found no noticeable difference in slope angle in rockslide and debris flow events. The highest occurrence of landslides was at slope angles between 25 – 42°. Identified rockfall-type events were tightly concentrated near the marine terrace system. This terrace system has a slope angle in general greater than 74° (see Figure 5a). Debris

flows and rockslides were triggered by hurricane Matthew mostly between 200 - 500 masl, while rockfall events were identified at heights lower than 45 masl, in the lower level of the terrace system near the shoreline.

Most of rockslide-type landslides were generated in materials composed by green schists of volcanic and vulcanoclastic rocks and rocks of the ophiolitic complex constituted by ancient remains of oceanic crust as shown in Figure 5c. Within its composition predominate harzburgites, lherzolites and serpentinized dunites of the Cretaceous Lower-Upper and Middle Jurassic as show Table 2. These are the oldest rocks in the study area and present different degrees of weathering and high deformation. Debris flows mostly occurred in rocks from the Middle Jurassic ophiolitic complex and in magmatic rocks and to a lesser degree in rocks composed of green schists of volcanic and vulcanoclastic rocks of Cretaceous age. Rockfalls were concentrated in the Maya formation composed of organodetrritic and organogenic limestones from the Upper Pliocene-Upper Pleistocene and the Jaimanitas formation composed of calcified bioterritic limestone from the Upper Pleistocene (Table 2).

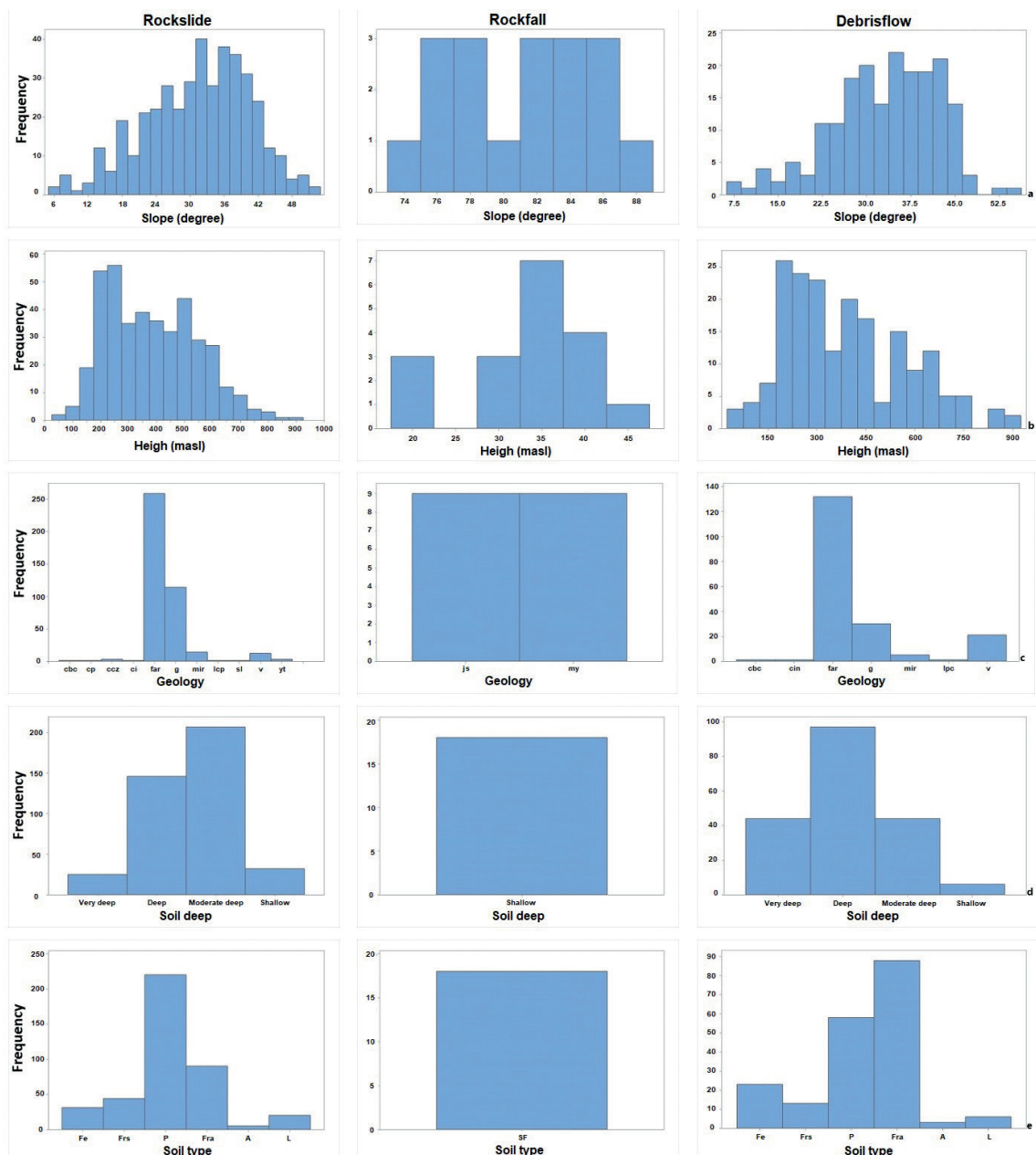


Fig. 5. Distribution landslide types taking into account the slope in degrees (a), height in masl (b), rock formations (c) geology (see table 2), soil depth (d) and soil type (e) where: Fe are ferritic soils; Fr fersialitic; P brown soils; Fra ferralitic soils; To alitic soils; L latosolic soils and IF soils in formation

Table 2. Relation of landslide occurrence with rock types

Unit name	Rock type	Age	Landslide type		
			rockslide	debrisflow	rockfall
Ofolitic Complex (g)	Rocks of the ophiolitic association: harzburgites, lherzolites, serpentized dunites	Middle jurassic	114	30	
Magmatic rocks (v)	Undifferentiated gabbroids, gabbros, and diabases		12	21	
Formation La Farola (far)	Green schists of volcanic and vulcanoclastic rocks	Lower Cretaceous- Upper Cretaceous	259	132	
Formation La Picota (lpc)	polymythic conglomerates interspersed with polymythic sandstones	Upper Cretaceous	1	1	
Formation Capdevila (cp)	conglomerates with sandstones and siltstones	Lower Eocene	1		
Formation Castillo de los Indios (cin)	volcanic rocks mainly tuffs	Lower-Middle Eocene		1	
Formation Miranda (mir)	conglomerates of tuff, tuff, and marl	Lower-Middle Eocene	14	5	
Formation San Luis (sl)	Stratifications of polymyctic sandstones, siltstones, marls	Middle Eocene- Upper Eocene	1		
Formation Yateras (yt)	biodetritic limestones alternated with biogenic limestones	Upper Oligocene	3		
Member Cilindro (ci)	Polymyctic conglomerates with lenticular stratification and sometimes crossed, weakly cemented, with sandstone lenses, containing lignite. The matrix is polymyctic sandstone, containing carbonate.	Upper Oligocene- Lower basal Miocene	1		
Formation Cabacú (cbc)	Gravelite, sandstones and siltstones	Upper Oligocene- Lower basal Miocene	1	1	
Formation Cabo Cruz (ccz)	Biodetritic limestones	Middle Miocene- Upper Miocene	3		
Formation Jaimanita	Massive biodetritic limestones, generally karst, very fossiliferous.	Upper Pleistocene.			9
Formation Maya (my)	Marine Deposits, Organodetritic and Organogenic Limestones.	Upper Pliocene-Upper Pleistocene			9

Other factors conditioning the occurrence of landslide events were considered, such as the depth and type of soil. According to the soil classification of the Cuban Soil Institute, 1973, in the study area Ferritic, Ferralitic, Fersialitic and Brown soils are common, which overlie ultrabasic and basic rocks with intense alteration and a high content of clay minerals.

A total of 358 of identified landslide events occurred over moderately deep soils (210) and in deep soils (148) with depth ranges from 20-50 cm to 50-100 cm respectively (Figure 4d). These figures are consistent with the predominance of shallow landslides. Regarding rockfall events, its distribution was on areas of shallow layers of soils in formation with less than 20 cm. A high number of rockslides were identified in areas of brown soils (53%) with a clay loam and sandy texture followed by ferralitic soils (17%) with a sandy loam and clay loam texture. However,

debris flows had a predominance in Ferralitic soils (46%) over Brown soils (31%) (Figure 5e).

Rain thresholds after Hurricane Matthew

The assessment of the relationship between landslides and rainfall during and immediately after the hurricane influence was one of the main goals of this study. After accounting for the spatial location and the radius of influence of the rain gauges, the research found that most of the landslides were concentrated in the areas affected by intense rainfall. Such findings confirm the relationship of the occurrence of landslides with intense rainfall found by other authors (Lumb 1975; Garland and Oliver 1993; Kay and Chen 1995; Finlay et al. 1997; Crosta 1998, 2003; Guzzetti 1998; Crozier 1999; Dai et al. 2001; Aleotti 2004; Dikshit et al. 2019; Sarkar and Dorji 2019).

The behavior of the accumulated (24 h) daily rainfall (AR) associated with the days of Hurricane Matthew influence over the study area (October 4th, 5th and 6th), the accumulated antecedent rainfall (AAR) for 3 and 15 days and the accumulated total over those days (Figure 6) were compared with the landslide inventory. This research found the majority of landslides were located near areas of significant rainfall accumulated. As can be seen in the Figure 6, the daily rainfall accumulations on day 6 (Figure 6c) and the previous rainfall accumulations for 3 and 15 days (Figure 6d and 6e) are not significant for the area, reporting values below 30 mm/d.

The definition of empirical or statistical thresholds is an excellent indicator for landslide forecast since it allows the association of the probability of landslide events with established weather forecast models. Accordingly, thresholds are important elements for designing landslide early warning systems along with other conditioning factors which may increase their effectiveness. To calculate the rainfall thresholds after the passage of Hurricane Matthew, the records of 10 mountain rain gauges located in the area were analyzed (see fig 1) and the existence of rain gauges with rainfall records that deviated from the accumulated rainfall trend in the period of the hurricane's passage. For the establishment of the rainfall thresholds, minimum accumulated rainfalls of 0.8-50 mm and

maximum accumulated rainfalls of 250-520 mm were analyzed. The computed thresholds for accumulated rainfall corresponding to day 4 are shown in Figure 7. The maximum threshold in which the highest percentage of landslide events occurs (88%) is between 355 mm and 178 mm. In the case of day 5, the maximum calculated threshold (82% of landslide events) was 407 mm and the minimum threshold 118 mm. The standard deviation is significantly higher for the rainfall records on day 5 due to the number of measurements with zero rainfall data, mostly by equipment failures, which creates higher uncertainty for the thresholds on this day (Figure 7d).

The thresholds for the combination of AR and AAR of 3 days were discarded because AR of less than 30 mm which is below intense rainfall accumulates.

This research found little evidence of influence of antecedent accumulated rainfall in landslide occurrence. The accumulated rainfall on October 4th and 5th are mostly the triggering factors of most landslides. The minimum thresholds calculated on these days could be indicative of the amount of rainfall above which the probabilities of occurrence of landslide events may drastically increase. These threshold values, along other conditioning factors, may be the foundation for setting up an early warning system for landslides in the region.

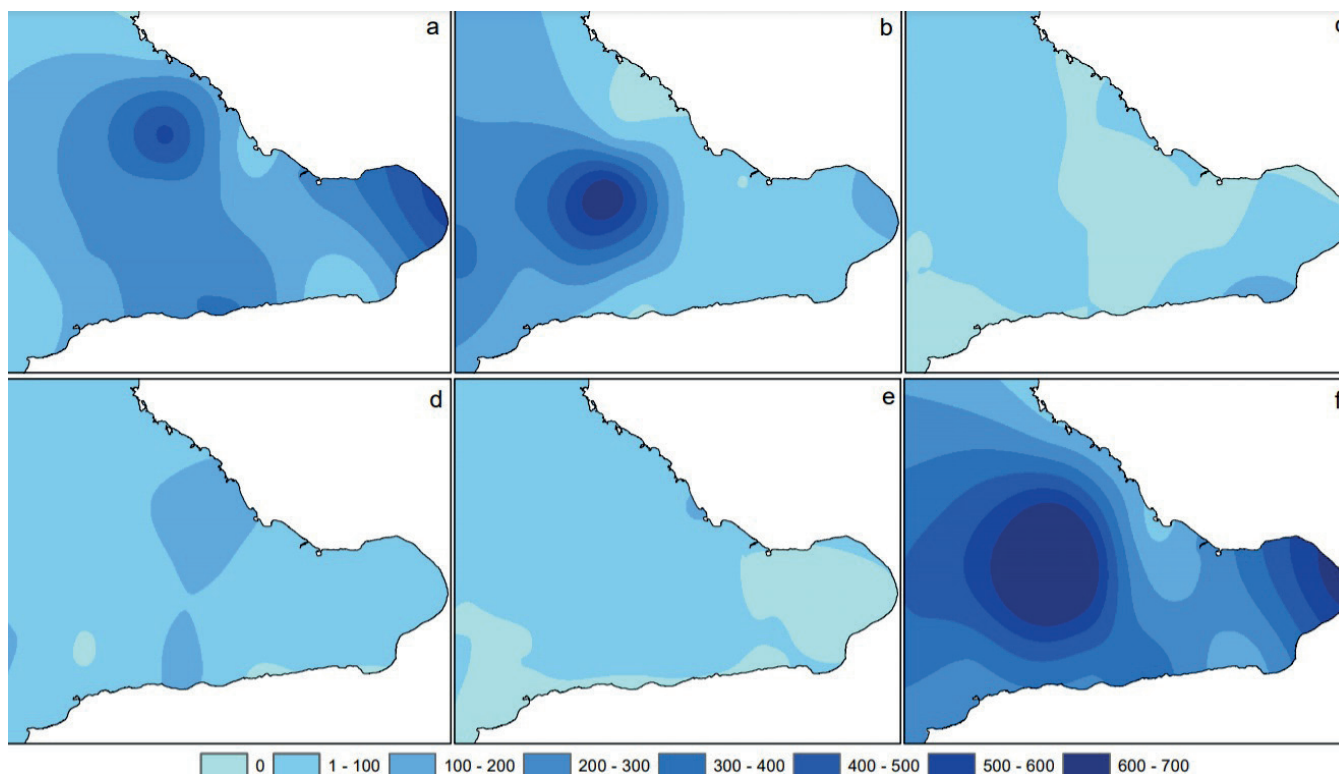


Fig. 6. Rainfall associated to Matthew hurricane and before (mm): a) October 4, 2016; b) October 5, 2016; c) October 6, 2016; d) accumulated rainfall 3 days before; e) accumulated rainfall 15 days before; f) Accumulated rainfall days 4, 5 and 6 October 2016

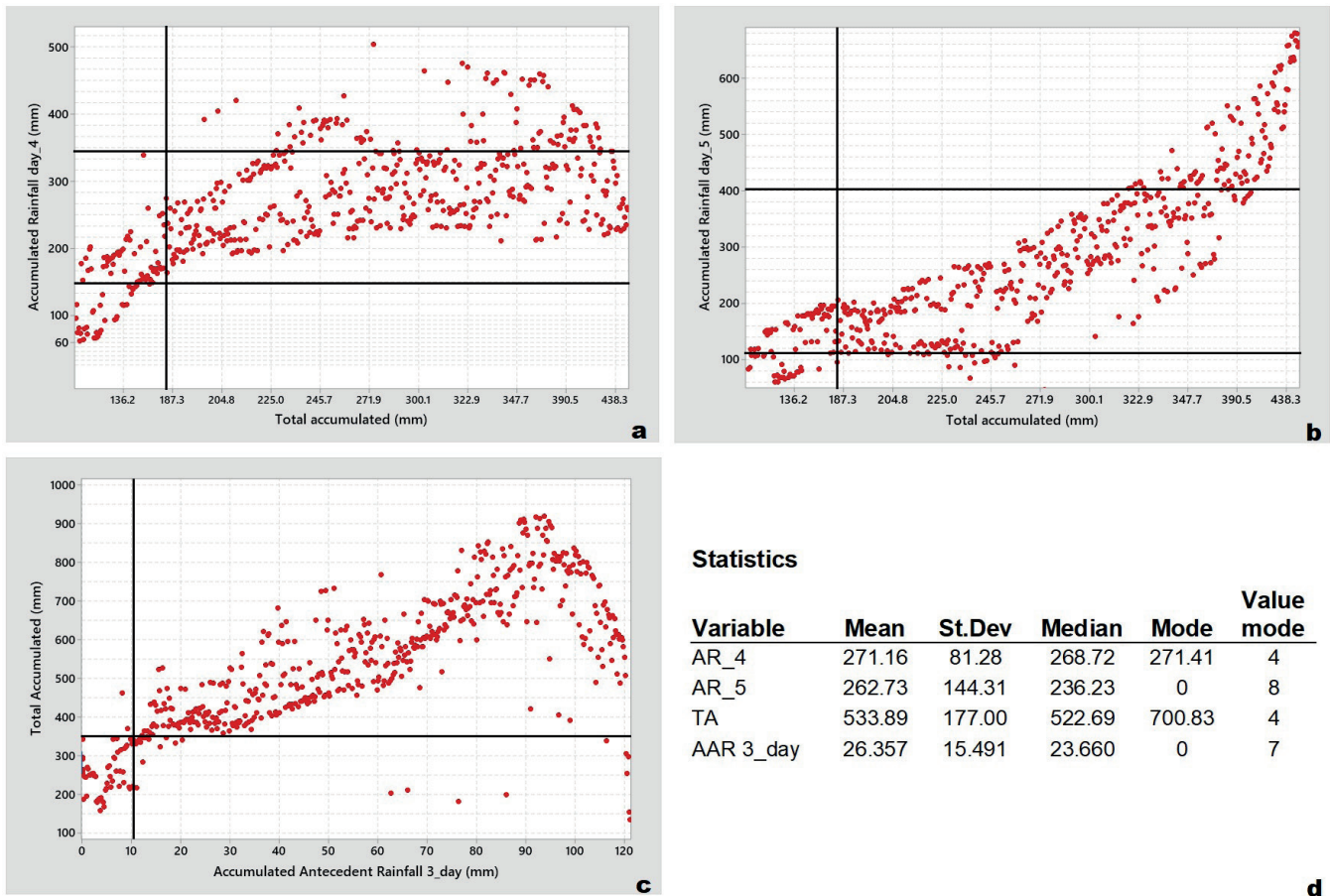


Fig. 7. Rainfall thresholds triggering landslides for Hurricane Matthew in the study area: a) rainfall threshold day 4; b) rainfall threshold day 5; c) rainfall threshold calculated considering 3 days of antecedent rainfall; d) statistics for accumulated rainfall and accumulated rainfall antecedents, where AR is the accumulated daily rainfall for day 4 (AR_4) and for day 5 (AR_5). TA is total accumulated rainfall throughout the passage of the hurricane. AAR 3_day is accumulated of antecedent rainfall for three days

CONCLUSIONS

Hurricane Matthew affected Guantánamo province in Eastern Cuba triggering 619 landslides as interpreted by satellite images and fieldwork. The majority of the landslides found were rockslides that occurred in the north-central part of the study area with a small amount of debrisflows and rockfalls. The areas with higher rainfall overlapped with highest landslide occurrence, except for intra mountain valleys, which is in accordance with the nature of the event. Most of the landslides identified were triggered on high and moderated hazard zones for the hazard map from previous research.

Slope angle does not seem to represent a factor as important as the rock type in the area, since many landslides

occurred in slopes lower than 45°. Debrisflow occurred mostly on deep ferralitic soils and rockslides on moderately deep brown soils. Most of landslides were located in green schists of volcanic and vulcanoclastic rocks, as well as rocks of the ophiolitic association: harzburgites, lherzolites and serpentized dunites.

Rainfall thresholds causing landslides during the passage of Hurricane Matthew are between 178-407 mm/d. The accumulated antecedent rainfall was not significant for the establishment of thresholds.

This landslide inventory contributes to previous efforts in reducing landslide risk in the mountain areas of Guantánamo province and are the base to updating landslide susceptibility and hazard maps in the region. ■

REFERENCES

- Aleotti P. (2004). A warning system for rainfall-induced shallow failures. *Engineering Geology*, 73, 247-265, DOI:10.1016/j.enggeo.2004.01.007.
- Aristizábal E. and Gómez J. (2007). Inventario de emergencias y desastres en el Valle de Aburrá. originados por fenómenos naturales y antrópicos en el periodo 1880-2007. *Gestión y Ambiente*, 10(2), 17-30, <https://revistas.unal.edu.co/index.php/gestion/article/view/1409>.
- Aristizábal E. and Yokota S. (2006). Geomorfología aplicada a la ocurrencia de deslizamientos en el valle de aburra. *DYNA*, 73(149), 05-16. <https://revistas.unal.edu.co/index.php/dyna/article/view/807>.
- Ayalew L. and Yamagishi H. (2005). The application of GISbased logistic regression for landslide susceptibility mapping in the Kakuda-Yahiko Mountains, Central Japan. *Geomorphology*, 65, 15-31, DOI:10.1016/j.geomorph.2004.06.010.
- Ballester M. and Rubiera J. (2016). Summary of cyclone season 2016 in North Atlantic, Institute of Meteorology (INSMET), Ministry of Science, Technology and Environment, Cuba, <http://www.insmet.cu/asp/genesis.asp?TB0=PLANTILLAS&TB1=TEMPORADA&TB2=/Temporadas/temporada2016.html#home>.
- Bertinelli L., Mohan P. and Strobl E. (2016). Hurricane Damage Risk Assessment in the Caribbean: An Analysis Using Synthetic Hurricane Events and Nightlight Imagery. *Ecological Economics*, 124, 135-144, DOI:10.1016/j.ecolecon.2016.02.004.
- Brown W.M., Cruden D.M. and Denison J.S. (1992). The directory of the world landslide inventory. USGS Open File Report 92 (427), 239.
- Castellanos E.A. and Van Westen C.J. (2007). Generation of a landslide risk index map for Cuba using spatial multi-criteria evaluation. *Landslides*, 4, 311-325, DOI:10.1007/s10346-007-0087-y.
- Castellanos E.A. and Van Westen C.J. (2008). Qualitative landslide susceptibility assessment by multicriteria analysis: A case study from San Antonio del Sur, Guantánamo, Cuba, *Geomorphology*, 94(3-4), 453-466, DOI:10.1016/j.geomorph.2006.10.038.
- Crosta G.B. (1998). Regionalization of rainfall thresholds: an aid to landslide hazard evaluation. *Environmental Geology*, 35, 131-145, DOI:10.1007/s002540050300.
- Crozier M.J. (1999). Prediction of rainfall-triggered landslide: a test of antecedent water status model. *Earth surface processes and landforms*, 24, 825-833, DOI:10.1002/(SICI)1096-9837(199908)24:9<825::AID-ESP14>3.0.CO;2-M.
- Dai F., Lee C., Li J., and Xu Z.W. (2001). Assessment of landslide susceptibility on the natural terrain of Lantau Island, Hong Kong. *Environmental Geology*, 40, 381-391, DOI:10.1007/s002540000163.
- Dashko R.E. and Kotiukov P.V. (2018). Fractured clay rocks as a surrounding medium of underground structures: The features of geotechnical and hydrogeological assessment. *Saint Petersburg*, 1, 241-248, <https://onepetro.org/ISRMEUROCK/proceedings-abstract/EUROCK18/All-EUROCK18/ISRM-EUROCK-2018-025/446888>.
- Dikshit A., Sarkar R., Pradhan B., Acharya S. and Dorji K. (2019). Estimating Rainfall Thresholds for Landslide Occurrence in the Bhutan Himalayas. *Water* 11, 1616, DOI: 10.3390/w11081616.
- Finlay P.J., Fell R. and Maguire P.K. (1997). The relationship between the probability of landslide occurrence and rainfall. *Canadian Geotechnical Journal*, 36, 811-824, DOI:10.1139/t97-047.
- Garland G.G. and Oliver M.J. (1993). Predicting landslides from rainfall in a humid, sub-tropical region. *Geomorphology*, 8, 165-173, DOI:10.1016/0169-555X(93)90035-Z.
- Gospodarikov A.P. and Zatselin M.A. (2010). Mathematical modeling of stress-strain state of the mined seam deposits. *Journal of Mining Institute*, 187, 47, <https://pmi.spmi.ru/index.php/pmi/article/view/6623>.
- Gusev V.N. (2016). Forecasting safe conditions for developing coal bed suites under aquifers on the basis of geomechanics of technogenic water conducting fractures. *Journal of Mining Institute*, 221, 638, DOI:10.18454/pmi.2016.5.638.
- Guzzetti F. (1998). Hydrological triggers of diffused landsliding. *Environmental Geology*, 2(35), 78-79.
- Guzzetti F., Cardinalli M., and Reichenbach P. (1994). The AVI project: a bibliographical and archive inventory of landslides and floods in Italy. *Environmental Management*, 18, 623-633, DOI: 10.1007/BF02400865.
- Iturralde-Vinent M.A. (1998). Sinopsis de la Constitución Geológica de Cuba». *Acta geológica hispánica*, 33, 9-56, <https://www.raco.cat/index.php/ActaGeologica/article/view/75545>.
- Kay J.N. and Chen T. (1995). Rainfall-landslide relationship for Hong Kong. *Proceeding ICE. Geotechnical Engineering* 113, 117-118, DOI: 10.1680/igeng.1995.27592.
- Kleptsova O.S., Dijkstra H.A., van Westen R.M., van der Boog C.G., Katsman C.A., James R.K., Bouma T.J., Klees R., Riva E.M., Slobbe D.C., Zijlema M. and Pietrzak J.D. (2021). Impacts of Tropical Cyclones on the Caribbean Under Future Climate Conditions. *Journal of Geophysical Research: Oceans*, 126(9), e2020JC016869, DOI:10.1029/2020JC016869.
- Kutepova N.A., Kutepov Y.I., and Shabarov A.N. (2012). Engineering-geological ensuring for safety of mining work in water-inundated solid mass. *Journal of Mining Institute*, 197, 197. извлечено от <https://pmi.spmi.ru/index.php/pmi/article/view/5991>.
- Kutepova N.A., Kutepov Y.I., & Shabarov A.N. (2012). The monitoring of hidrogeomechanical processes during the flooding of Angero-Sudgensk mines. *Journal of Mining Institute*, 197, 215, <https://pmi.spmi.ru/index.php/pmi/article/view/5994>.
- Lumb P. (1975). Slope failure in Hong Kong. *Quarterly Journal Engineering Geologist*, 8, 31-65, DOI: 10.1144/GSL.QJEG.1975.008.01.02.
- Marcelino E.V., Fromaggio A.R. and Maeda E.E. (2009). Landslide inventory using image fusion techniques in Brazil, *International Journal of Applied Earth Observation and Geoinformation*, 11, 181-191, DOI: 10.1016/j.jag.2009.01.003.
- Posphehov G.B., Straupnik I.A. and Pankratov K.V. (2018). Geoengineering researches for the restoration of the lands disturbed by mining. 14th Conference and Exhibition on Engineering and Mining Geophysics, vol. 2018, № 137600, 1-5, DOI: 10.3997/2214-4609.201800528.
- Ranson M., Kousky C., Ruth M., Jantarasami L., Crimmins A. and Tarquinio L. (2014). Tropical and Extratropical Cyclone Damages under Climate Change. *Climatic Change*, 127(2), 227-41, DOI: 10.1007/s10584-014-1255-4.
- Sarkar R. and Dorji K. (2019). Determination of the Probabilities of Landslide Events—A Case Study of Bhutan. *Hidrology*, 6(2), 52, DOI: 10.3390/hydrology6020052.
- Stedinger J.R. (1993). Frequency analysis of extreme events. In: Maidment DR (ed) *Handbook of Hydrology*. McGraw-Hill: New York., 18.1-18.66.
- Trushko V.L., and Protosenya A.G. (2019). Prospects of geomechanics development in the context of new technological paradigm. *Journal of Mining Institute*, 236, 162, DOI: 10.31897/pmi.2019.2.162.
- Van Westen C.J., Castellanos E.A. and Kuriakose S.L. (2008). Spatial data for landslide susceptibility, hazard and vulnerability assessment: an overview. *Engineering Geology*, 102(3-4), 112-131, <https://www.sciencedirect.com/science/article/abs/pii/S0013795208001786>.